Fullerene derivatives and aluminum-based nanothermites as potential new ammunition primers

Prepared by:
Daniel Chamberland
Chemist
NUMERICA TECHNOLOGIES INC

Prepared for:
Catalin Florin Petre
418-844-4000
DRDC Valcartier

Contract number:
W7701-103156/001/QCL

Defence Research and Development Canada

Fullerene derivatives and aluminum-based nanothermites as potential new ammunition primers

Daniel Chamberland

NUMERICA TECHNOLOGIES INC

March 28, 2013

Table of contents i

Part A: Fullerenol

1. BACKGROUND

The possibility to ignite a material with a low-energy irradiation is very interesting and may have applications in the ignition systems of gunpowder. In 2002, it was demonstrated that certain types of carbon nanotubes (SWNT) (Fig.1) could burn by simple exposure to a conventional photographic flash [1].
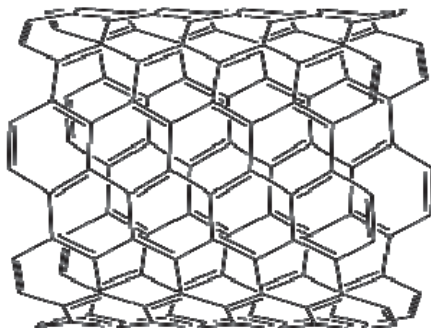
Figure 1: Structure of single wall nanotube (SWNT)

Then in 2010, it has been shown that derivatives of fullerene (C_{60}) can be heated to the point of ignition by laser irradiation of low intensity [2]. The ignition is achieved by irradiation in the near infrared (785 nm) as well as green light (540.5 nm) and blue light (488 nm) at intensities as low as 100W/cm^2. The fullerene derivative compound that appeared to be the most attractive was polyhydroxyfullerene $C_{60}(OH)_n$ or fullerenol (Fig.2).
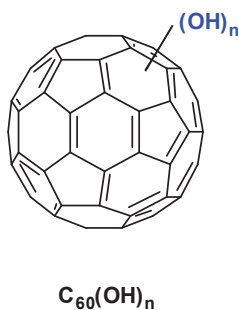
$C_{60}(OH)_n$

Figure 2: Structure of polyhydroxyfullerene $C_{60}(OH)_n$

The company *BuckyUSA* commercializes fullerenes and fullerenol. The cost for 10 grams of the C_{60} fullerene is 250.00 USD while the derivative fullerenol marketed with the molecular formula $C_{60}(OH)_{18-22}$ is much more costly at 1000.00 USD for 1 gram thus 40 times more expensive. Was acquired 1 gram of fullerenol $C_{60}(OH)_{18-22}$ for its characterization and to perform some ignition tests and 10 grams of fullerene C_{60} to develop a methodology for the production of fullerenol at a lower cost.

1.   2.   PREPARATION OF FULLERENOL

Fullerenol synthesis as reported in the literature is mainly based on three approaches. The first one relies on the action of a concentrated sodium hydroxide solution on fullerene in organic solution using a phase transfer agent (TBAH) such as illustrated in Fig. 3.
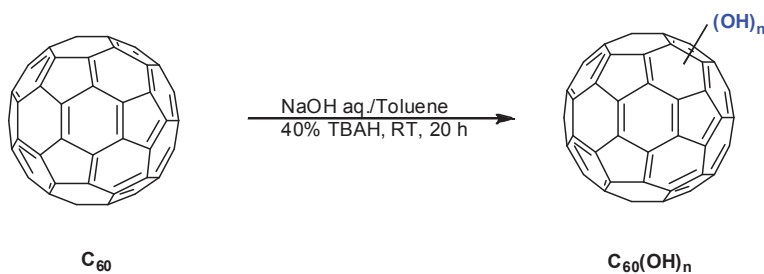
Figure 3: Synthesis of fullerenol with sodium hydroxide (NaOH)

The authors of many of these procedures have concluded that the resulting compound formed was the hydroxylated product with a hydroxyl number from 12 to 36 depending on the reaction time, temperature and the number of equivalent NaOH used. However, more recent studies have shown that the products obtained by this method are essentially sodium salts like $Na_n^+[C_{60}O_xOH_y]_n^-$ and most procedures are poorly reproducible and lead to mixtures of different molecular structures and the composition is variable from one batch to another. [3]

The second approach for the synthesis of fullerenol is based on the reaction of fullerene with hydrogen peroxide in organic solution with the presence of a phase agent (Fig. 4). This approach has been only been used by the group of Kokubo [4]. Here too, this synthesis leads to the formation of several derivatives with the presence of epoxides (C-O-C) and carbonyl group (-C = O) involving ring opening.
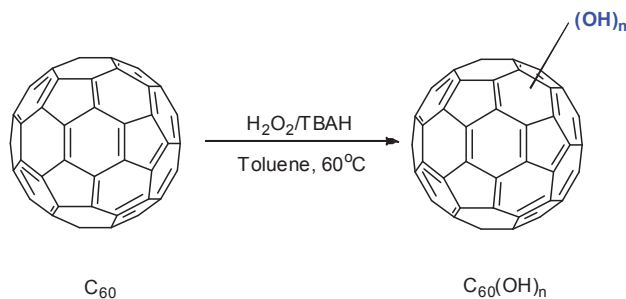
Figure 4: Synthesis of fullerenol with hydrogen peroxide (H_2O_2)

The third method for the synthesis of fullerenol takes place in two steps [5]. First the fullerene is brominated by the action of bromine in the presence of iron as a catalyst. The derivative obtained has the formula $C_{60}Br_{24}$. The bromine derivative is then subjected to the action of sodium hydroxide to provide fullerenol $C_{60}(OH)_{24}$ (Fig. 5).
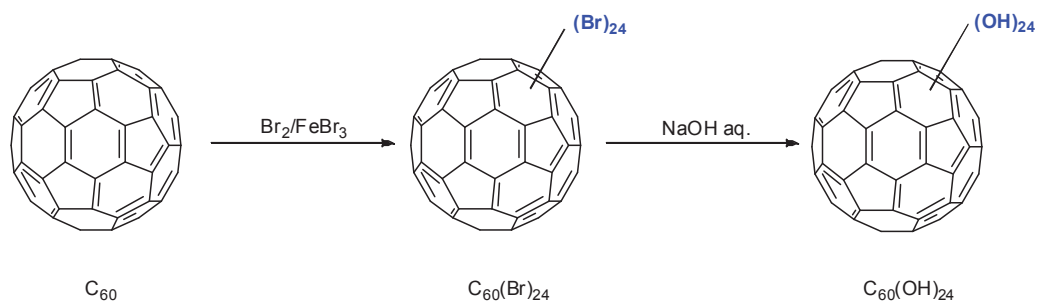
Figure 5: Synthesis of fullerenol in two steps

3. EXPERIMENTAL

3.1 Oxidation with hydrogen peroxide

The first tests for the synthesis of fullerenol were based on the method using oxidation with hydrogen peroxide in the presence of tetrabutylammonium hydroxide (TBAH) as a phase transfer agent as described in the following procedure.

C_{60} $C_{60}(OH)_n$
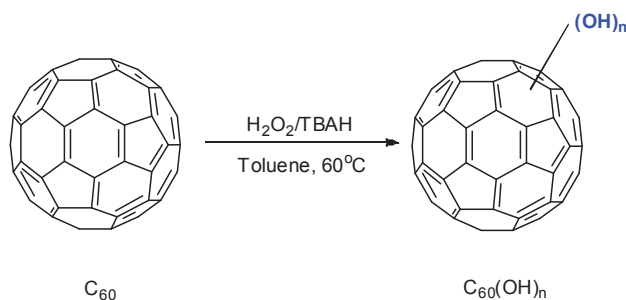
PHF-001	F.W.	Mass (g)	mmol	Vol (mL)	Eq.
Fullerene (C_{60})	720.64	0.5	0.694	0.5	1
H_2O_2 (30%)	34.01	16.518	0.486	49.6	700
TBAH (40%)	259.47	1.008	3.885	2.52	5.6
Toluene				250	

To a toluene solution (250 mL) of C_{60} (0.500 g) was added a 30% H_2O_2 aqueous solution (49.6 mL) and TBAH (40% in water, 2.52 mL) and the mixture stirred for 24 h at 60 °C in air until the purple toluene layer turned into a colorless transparent solution leaving a yellowish aqueous phase (Fig 6). After cooling the mixture, the aqueous solution (ca. 50 mL) was separated and a mixed solvent of 2-propanol, diethyl ether, and hexane (7:5:5, 500 mL) was added to yield a milky white precipitate. After centrifugation and decantation the solid residue was washed with diethyl ether by ultrasonic-centrifuge-decantation procedure. Drying the residue under vacuum gave 64 mg of a brown solid. Assuming that the average number of hydroxyl groups is 30, the molecular weight of the final product would be 1230 g/mol. The 64 mg of product obtained therefore reflect a very low yield of 7-8%. Analysis of the residue by proton NMR in solution in D_2O clearly indicates the presence of TBAH. With carbon-13 NMR spectra, it was impossible to see other signals than those attributed to TBAH. It was not possible to purify the solid by the procedure of dissolution in water and precipitation with a of low polarity solvent mixture as described by Kokubo [4]

Figure 6: Color changes in the oxidation of fullerenol after: A) one hour, B) 8 hours and C) 24 hours

Several other attempts were made for the preparation of fullerenol by oxidation with hydrogen peroxide. Was varied the number of equivalent of hydrogen peroxide and of TBAH, the nature of the reaction solvent (benzene, 1,2,4-trimethylbenzene) and mixtures of various solvents for the precipitation of the fullerenol in the aqueous phase. None of these changes have provided the expected product. The only product that has been identified by NMR in these trials is the phase transfer agent TBAH. An extensive literature review has not been successful to find other procedures using hydrogen peroxide for the preparation of fullerenol.

3.2 Treatment of fullerene with sodium hydroxide

A review of the literature on the preparation of fullerenol indicates that the main route of synthesis is the hydroxylation of fullerene with concentrated sodium hydroxide solution in the presence of phase transfer agent. The following procedure is representative of the various tests performed for the preparation of fullerenol.
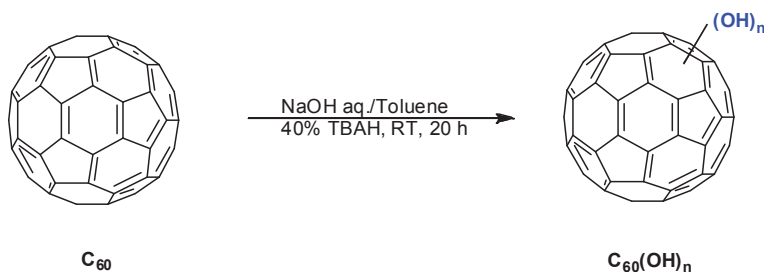
Reagents	F.W.	Mass (g)	mmol	Vol (mL)	Eq.
Fullerene (C$_{60}$)	720.64	*0.100*	0.139	0.100	1
NaOH (50%)	40.00	*2.498*	62.444	*2.498*	450
TBAH (40%)	259.47	*0.151*	0.583	*0.378*	4.2
Benzene				*75*	

C$_{60}$ (0.1 g) was added to benzene (75 mL) and the mixture was stirred for 30 minutes. Then, 2.5 mL of NaOH solution (50%) was added with 0.378 mL of TBAH (40% in water). The mixture was stirred rapidly for 4 hours and the purple coloration of organic phase disappeared leaving a dark precipitate. Benzene

was removed by decantation and to the aqueous phase, water (25 mL) was added and the solution was stirred for an additional 24 hours. The suspension was then passed through a paper filter to remove the suspended solids. The filtrate was then concentrated in a vacuum oven at 60°C for 24 h. The remaining brown wet solid was then washed three times by repeated centrifugations at 2000 rpm for 10 minutes with 50 mL methanol each time and finally dried in vacuum at room temperature for 24 h. The weight of the dried fullerenol obtained was 103 mg. By assuming a molar weight of 1230 g/mol for fullerenol, the yield obtained with 103 mg is approximately 55-60%. The characterization of the product obtained by NMR is inconclusive. The product is soluble only in water thus making the proton NMR unhelpful since the expected signals for hydroxyl groups are masked by deuterium exchange with the solvent. However, we can still detect the presence of the phase transfer agent TBAH. As fullerenol obtained is a mixture of different hydroxylated product, there are numerous types of different quaternary carbon atoms, making the carbon-13 NMR unhelpful.

3.3   Bromide derivative of fullerene C_{60}

The last proposed method for the synthesis of fullerenol is the hydrolysis of the bromide derivative of fullerene by the action sodium hydroxide. The brominated derivative was prepared by bromination of fullerene with the iron bromide ($FeBr_3$) as catalyst [6]. The catalyst is generated in situ by reaction between iron and bromine.

$$C_{60} \xrightarrow{Br_2/FeBr_3} C_{60}(Br)_{24}$$
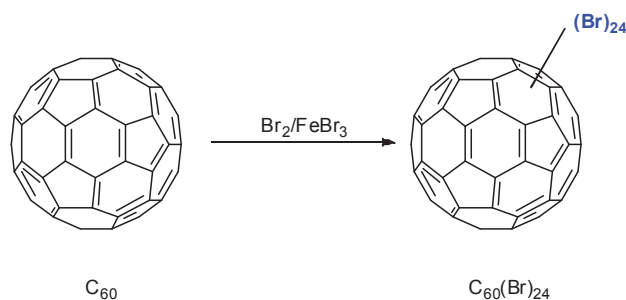
Reagents	F.W.	Mass (g)	mmol	Vol (mL)	Eq.
Fullerene (C_{60})	720.64	0.050	0.069	0.050	1
Bromine	159.81	15.514	97.078	5.00	116.5969

In a 10 mL round bottom flask, neat bromine (5 mL) was added to 50 mg C_{60} and a large-gauge iron wire (1 mm dia. X 1 cm length). The mixture was stirred vigorously at room temperature for one hour, after which the excess liquid bromine was removed by evaporation under an air stream. The resulting dark solid was treated with 20 mL of methanol, a procedure that dissolves the ferric bromide that forms during the reaction. The iron wire was removed, and the methanol mixture was filtered to give a yellow powder, which was washed with additional methanol. The solid was finally washed with diethyl ether and dried under reduced pressure. The yield of the bromide derivative was 190 mg (97.9%). the hydrolysis step has not been done since like the previous method, the hydrolysis product would have been contaminated with sodium and purification method was not adequate.

3.4   Purification of fullerenol

As discussed previously, the method employing sodium hydroxide leads to mixtures of hydroxylated products and species contaminated with sodium. Recently, purification procedures to get rid of the sodium content from fullerenol obtained from NaOH solution have been reported [7]. The purification is based on exhaustive washing with deionized water, followed by precipitation with methanol before final purification by ion-exchange chromatography with Amberlit MB-20 resin. This material was not available at the time of synthesis of fullerenol.

3.5   SEM characterization of and laser ignition test of fullerenol

The product obtained by the method with sodium hydroxide and the commercial product sold as fullerenol $C_{60}(OH)_{18-22}$ were subjected to scanning electron microscopy (SEM). Results are in good agreement with the literature and clearly show that the commercial product and the product synthesized in the laboratory are heavily contaminated with sodium (Fig. 7).
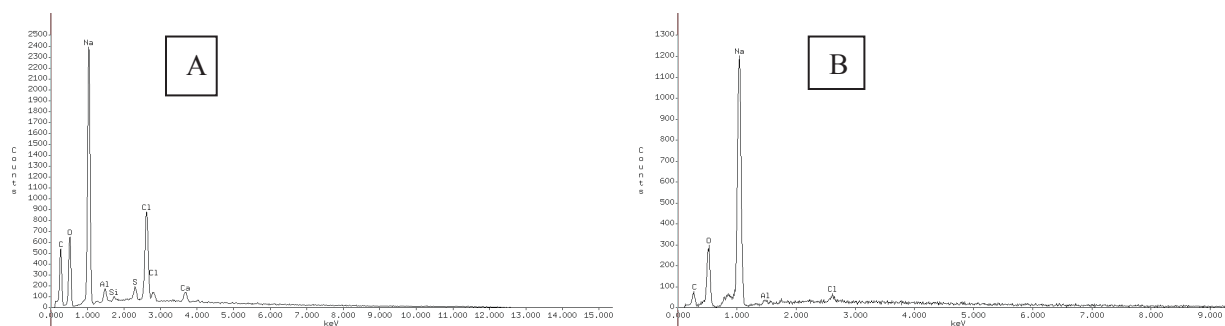
Figure 7: SEM spectrum of commercial fullerenol (A) and fullerenol synthesized in the laboratory (B)

Testing the laser ignition of the two samples was carried out with a blue laser (445 nm) at a power of 1.7W. The results are identical for both samples. There is no propagation of the ignition outside the area illuminated by the laser. Samples ignite only where the laser strikes leaving intact the material around the area exposed to laser. For more details on the setup for laser ignition test see Tommy Ringuette report

4.   CONCLUSION

 Of the above, it is clear that we cannot draw any conclusion regarding the possibility of laser ignition of fullerenol. It has not been possible to obtain pure fullerenol free of sodium salt as contaminant. The commercial product sold as $C_{60}(OH)_{18-22}$ is also contaminated with sodium salt as demonstrated by SEM analysis. To do this, the purification by chromatography should be carried out as discussed above. This is a time consuming and expensive process and does not guarantee in any way that purified fullerenol will behave differently in laser ignition.

The scientific literature on the use of fullerene derivatives as energetic material is virtually nonexistent. The only clear example is described in a 2006 patent [8] on the preparation and performance of the nitrofullerene derivative $C_{60}(NO_2)_{12}$.

DRDC-RDDC-2014-C39

Part B: Aluminum-based nanothermites

1.   Background

The spectrum of physicochemical properties offered by nanothermites by changing their compositions, allow considering a wide range of applications. Many of these applications arise directly from high energy density leading to applications such as microscale propulsion and nanoscale welding. One of the applications we are interested in specifically is their potential as ammunition primers and electric igniter and the possibility to ignite such a primer by low-energy laser irradiation. Traditional primers contain lead compounds such as lead azide and lead styphnate which are toxic for both personal user and the environment. The use of non-toxic nanothermites in this context would also be a benefit as a substitute for the various formulations containing lead or other toxic substances.

Nanothermites occupy an important place in research on energetic materials. This is largely due to high energy densities and adiabatic flame temperature, which are comparable to conventional organic energetic materials such as RDX. In a thermite type reaction, a metal oxide is the oxidant and the fuel is aluminum. The nanothermites are generally composed of aluminum and metal oxide nanopowders, unlike conventional thermite used for several years, which are composed of micron-sized powders. The rate of release of energy in conventional thermite is relatively slow in comparison with conventional energetic materials. The typical velocity of propagation of combustion front is of the order of a few centimeters to a few meters per second. A significant reduction in the particle size of the reactants (aluminum and metal oxide) leads to an important increase in the burning rate with some explosive behavior [9].

The thermite reaction between aluminum and a metal oxide leads to the formation of aluminum oxide and metal with release of energy according to the following reaction:

$$M_xO_y \quad + \quad Al \quad \rightarrow \quad M \quad + \quad Al_2O_3 \quad + \quad \Delta H \quad (1)$$

Table 1 presents some thermodynamic properties of some of the most studied nanothermites: theoretical maximum density (TMD), heat of reaction, amount of gas produced and the adiabatic reaction temperature [11].

Table 1: Thermodynamic properties oh selected thermite reactions

Thermite reaction	ρ_{TMD} [g/cm^3]	Q [cal/g]	Q [cal/cm^3]	Gas generation 1 atm [g gas/g mixture]	T_{ad} [K]
$2Al + Fe_2O_3 \rightarrow 2Fe + Al_2O_3$	4.175	945.4	3947	0.0784	3135
$2Al + Bi_2O_3 \rightarrow 2Bi + Al_2O_3$	7.188	505.1	3638	0.894	3319
$2Al + MoO_3 \rightarrow Mo + Al_2O_3$	3.808	1124	4279	0.2473	3688
$2Al + WO_3 \rightarrow W + Al_2O_3$	5.458	696.4	3801	0.1463	3253
$2Al + 3CuO \rightarrow 3Cu + Al_2O_3$	5.109	974.1	4976	0.3431	2843

Mixtures of aluminum and metal oxide are stable up to their ignition temperature at which point self-propagating high temperature synthesis takes place and the thermodynamic products of alumina (Al_2O_3) and metal are formed. Several models suggest as an explanation that the melting point of nanoparticle is significantly reduced, up to 300K lower than the micrometric material. This may have a major impact on the ignition temperature of thermite. For example, a mixture composed of 100 nm MoO_3 and 40 nm aluminum shows an ignition temperature of 458°C, while with the same MoO_3 and 10-14 µm aluminum exhibits an ignition temperature of 955°C [10]. In addition, the homogeneity of mixtures of nanoscale particles is higher. The surface to volume ratio increases considerably at nanoscale level and allows more of aluminum in contact with the metal oxide. Since the thermite reaction is partially controlled by diffusion, increasing the amount of aluminum in contact with the metal oxide reduces the diffusion distance and increases the rate of reaction.

In this section, will be reported the preparation of various nanothermite mixtures and results of sensitivity to electrostatic discharge (ESD), sensitivity to impact and friction and initial results with laser ignition tests.

2.   *Preparation of aluminum-based nanothermites*
2.

2.1   Safety aspects
Nanothermites are primary explosives and as such require special attention. In general, the smaller the particles are, the higher the sensitivity of thermite mixtures to impact and friction will be. Thermite mixtures at the microscopic level are generally not very sensitive to impact and friction, but at nanoscale, thermites can be very sensitive to either stimuli or one of the two depending on the nature of the metal oxide in the mixture.

Although the increased sensitivity can make the handling of nanothermites more dangerous, increased sensitivity to impact and friction can be beneficial in certain applications such as percussion primers. However, some thermites also have increased sensitivity to electrostatic discharge, which has no practical applications and therefore becomes a safety hazard. For example, the thermite composed of 40 nm Bi_2O_3 and 41 nm aluminum has a very high sensitivity to ESD and can ignites with only 0.125 µJ [9]. This energy level is well below what a human body can store making handling hazardous.

2.2   Composition of nanothermite mixtures
Thermite compositions are generally achieved by mixing powders of metallic oxide and aluminum in a specific mass ratio. The variation in the aluminum/metal oxide composition is reported in terms of equivalence ratio (φ):

$$\varphi = (F/A)_{Act}/(F/A)_{St} \tag{2}$$

In this equation, F represents fuel (Al), A is the oxidizer (metal oxide), and the subscripts *Act* and *St* indicate the actual and stoichiometric ratios. This equation considers the actual _active_ Al content. It is understood that $\varphi < 1$ corresponds to fuel lean mixtures, $\varphi > 1$ are fuel rich and $\varphi = 1$ are stoichiometric.

To start this project, the equivalence ratio was set at φ = 1.2 which is a slightly fuel rich mixtures. This choice reflects the recent literature where the value of 1.2 seems to be an optimal value for certain characteristics of nanothermites such as short delay of ignition and fast burning rate [10].

2.3   Material

The characteristics and performances of a thermite are closely related to the type of metal oxides and aluminum nanopowders, their geometric shapes (sphere, platelets), their dimensions, the equivalence ratio and the homogeneity of the mixture.

The type of aluminum that has been selected for the first mixtures is L-ALEX, an aluminum nanopowder coated with palmitic acid from *APT Metal Powder* (Tomsk, Russia). The average particle size is approximately 90-110 nm. Single particles have the average size of 70-150 nanometers and form micro agglomerates. The bulk density is about 0.32-0.37 g/cm3. BET surface area is 12 m^2/g. Whatever the type of aluminum used, the value of active aluminum content must be known. In fact, aluminum is always covered with a layer of aluminum oxide (Al_2O_3), and may also be covered with an additional coating. The determination of the active aluminum content was obtained by volumetric analysis based on the following chemical reaction: $2Al + 2NaOH + 2H_2O \rightarrow 2H_2 + 3NaAlO_2$. In carrying out the reaction in a fixed volume, the pressure change will be proportional to the amount of hydrogen released and itself proportional to the amount of active aluminum. The result for the active aluminum content L-Alex is 87.9%, which is consistent with the specifications of the supplier.

Among the different types of metal oxide nanopowders available, copper oxide (CuO), molybdenum oxide (MoO_3) and bismuth oxide (Bi_2O_3) were selected. Shape and dimension of the metal oxide nanopowders from *SkySpring Nanomaterials, Inc. (Houston, USA)* are given in Table 2.

Table 2: Shape and dimension of metal oxide nanopowders

Metal oxide	Shape	Size (nm)
CuO	Spherical	40
MoO_3	Spherical	100
Bi_2O_3	Spherical	<200

2.4   Mixing methods

The initial mixtures were prepared according to a widely used method, which involves mixing in a container the metal oxide and aluminum nanopowders in an inert solvent and placing the container in an ultrasonic bath for several minutes to ensure the homogeneity of the mixture. Thereafter, the mixture is left in a fume hood to allow the solvent to evaporate. This method is simple, but requires the use of flammable and volatile solvents such as hexane or isopropanol. In addition, when the mixture is dry, the surface layer tends to form aggregates that are somewhat difficult to break taking into account the sensitivity of nanothermites to friction. A second method was subsequently used and does not involve the use of solvent. A recent acquisition of a mixer at the experimental complex can mix powders of different nature using low frequency, high-intensity acoustic energy creating a uniform shear field

throughout the entire mixing container (Fig. 8). The LabRAM mixer is a product from *Resodyn Acoustic Mixers, Inc.* Since nanothermites are extremely sensitive to electrostatic discharge, the conductive container is grounded in order to prevent the accumulation of static electricity.

Figure 8: Picture of the mixer used for nanothermites preparation

3.   Experimental

3.1   Preparation of nanothermites with hexane and ultrasonic mixing

3.1.1   Al/CuO nanothermite

2Al + 3CuO → Al₂O₃ + 3Cu			
	FW	Weight (mg)	Mmol
Al (active)	26.982	77.2	2.514
Actual Al		*87.8*	
CuO (40 nm)	79.545	*250.0*	3.143
Total mass		337.8	
Mass Ratio $_{Act}$		0.309	
Mol Ratio $_{Act}$			0.800
Mass Ratio $_{st}$		0.226	
Mol Ratio $_{st}$			0.667
Hexane (mL)		*6.2*	
Equivalence ratio ϕ		1.200	
Lot number: LAXCU-001-1.2			

Wearing glasses and use an anti-static wristband is essential to avoid any incident relating to static electricity given the sensitivity of nanothermites to ESD.

In a glass tube was placed copper oxide (250 mg). Then was added hexane 6.2 mL and the mixture was sonicated for one minute to soak the copper oxide powder in the solvent. Aluminum L-ALEX (87.8 mg)

with an active content of 87.9% was added to the copper oxide/hexane mixture and the suspension was sonicated for 30 minutes. Temperature of water in the ultrasonic bath rose from 20°C to 35°C in that period of time. The suspension appeared as uniform slurry. The slurry was poured in a conductive container. The container was placed in a grounded metal drying pan in a fume hood until constant weight.

The dry powder is gently scraped from the wall of the conductive container; the container is then sealed and put in an appropriate place. The yield of recovery of Al/CuO nanothermite is 301 mg (97%). Losses are due to the powder remained stuck to the wall of the glass tube during sonication. L-ALEX powder is dark gray while CuO is black. The Al/CuO nanopowder is also dark gray.

Another preparation of Al/CuO nanothermite (Lot number: **LAXCU-002-1.2**) was prepared following exactly the same procedure.

3.1.2   Al/MoO3 nanothermite

$2Al + MoO_3 \rightarrow Al_2O_3 + Mo$			
	FW	**Weight (mg)**	**Mmol**
Al (active)	26.982	102.4	3.335
Actual Al		116	
MoO$_3$ (100 nm)	143.938	200	1.389
Total mass		*316*	
Mass Ratio $_{Act}$		0.512	
Mol Ratio $_{Act}$			2.400
Mass Ratio $_{st}$		0.375	
Mol Ratio $_{st}$			2.000
Hexane (mL)		5.80	
Equivalence ratio ϕ		1.200	1.20
Lot number: LAXMO-001-1.2			

In a glass tube was placed molybdenum oxide (200 mg). Then was added hexane (5.8 mL) and the mixture was sonicated for one minute to soak the molybdenum oxide powder in the solvent. Aluminum L-ALEX (116 mg) with an active content of 87.9% was added to the molybdenum oxide/hexane mixture and the suspension was sonicated for 30 minutes. Temperature of water in the ultrasonic bath rose from 22°C to 34°C in that period of time. The suspension appeared as uniform slurry. The slurry was poured in a conductive container. The container was placed in a grounded metal drying pan in a fume hood until constant weight.

The dry powder is gently scraped from the wall of the conductive container; the container is then sealed and put in an appropriate place. The yield of recovery of Al/MoO$_3$ nanothermite is 263 mg (83%). Losses are due to the powder remained stuck to the wall of the glass tube during sonication. L-ALEX powder is dark gray while MoO$_3$ is pale gray. The Al/MoO$_3$ nanopowder is also dark gray.

Another preparation of Al/MoO$_3$ nanothermite (Lot number: **LAXMO-002-1.2**) was prepared following exactly the same procedure.

3.1.3   Al/Bi$_2$O$_3$ nanothermite

2Al + Bi$_2$O$_3$ → Al$_2$O$_3$ + 2Bi			
	FW	**Weight (mg)**	**Mmol**
Al (active)	26.982	39.5	1.288
Actual Al		45.0	
Bi$_2$O$_3$ (200 nm)	465.959	250.0	0.537
Total mass		295.0	
Mass Ratio $_A$		0.158	
Mol Ratio $_A$			2.400
Mass Ratio $_s$		0.116	
Mol Ratio $_s$			2.000
Hexane (mL)		5.40	
Equivalence ratio ϕ		1.200	1.20
LAXBI-001-1.2			

In a glass tube was placed bismuth oxide (250 mg). Then was added hexane (5.4 mL) and the mixture was sonicated for one minute to soak the bismuth oxide powder in the solvent. Aluminum L-ALEX (45 mg) with an active content of 87.9% was added to the bismuth oxide/hexane mixture and the suspension was sonicated for 30 minutes. Temperature of water in the ultrasonic bath rose from 22°C to 35°C in that period of time. The suspension appeared as uniform slurry. The slurry was poured in a conductive container. The container was placed in a grounded metal drying pan in a fume hood until constant weight.

The dry powder is gently scraped from the wall of the conductive container; the container is then sealed and put in an appropriate place. The yield of recovery of Al/Bi$_2$O$_3$ nanothermite is 263 mg (83%). Losses are due to the powder remained stuck to the wall of the glass tube during sonication. L-ALEX powder is dark gray while Bi$_2$O$_3$ is a yellow powder. The Al/Bi$_2$O$_3$ nanopowder is greenish gray.

Two other preparation of Al/Bi$_2$O$_3$ nanothermite (Lot number: **LAXBI-002-1.2** and **LAXBI-003-1.2**) were prepared following exactly the same procedure.

3.2 Preparation of nanothermites with LabRAM mixer

3.2.1 Al/CuO nanothermite

2Al + 3CuO → Al$_2$O$_3$ + 3Cu			
	FW	**Weight (mg)**	**Mmol**
Al (Active)	26.982	77.2	2.514
Actual Al		*87.8*	
CuO (40 nm)	79.545	*250.0*	3.143
Total mass		*337.8*	
Mass Ratio $_A$		0.309	
Mol Ratio $_A$			0.800
Mass Ratio $_s$		0.226	
Mol Ratio $_s$			0.667
Equivalence ratio ϕ		1.200	1.20
Lot number: LAXCU-003-1.2-RAM			

Warning: wearing glasses and use of an anti-static wristband is essential to avoid any incident relating to static electricity given the sensitivity of nanothermites to ESD.

In a small conductive container was placed CuO (250 mg) and L-ALEX (87.8 mg). The container was capped with a rubber stopper. The container was attached with a metallic hose clamp which was used to ground the system (Fig. 9). The bottle was placed in the LabRAM mixer, grounded and the mixing rate was set as follows: 10% intensity for a period of 10 seconds and at 30% intensity for 30 seconds. The mixing was done in remote control. Visually, the mixture appeared homogeneous. The Al/CuO nanothermite was placed in a conductive container and stored. Another preparation of Al/CuO nanothermite (Lot number: **LAXCU-004-1.2-RAM**) was prepared following the same procedure but starting from 750 mg of CuO and 263 mg of L-ALEX to yield 1.013 g of nanothermite. The time of mixing at 30% intensity was also increased to 60 seconds.

Figure 9: Conductive bottle with stopper and hose clamp

3.2.2   Al/MoO3 nanothermite

$2Al + MoO_3 \rightarrow Al_2O_3 + Mo$			
	FW	**Weight (mg)**	**Mmol**
Al	26.982	128.0	4.168
Actual Al		146	
MoO$_3$ (100 nm)	143.938	250	1.737
Total mass		*396*	
Mass Ratio $_A$		0.512	
Mol Ratio $_A$			2.400
Mass Ratio $_s$		0.375	
Mol Ratio $_s$			2.000
Equivalence ratio ϕ		1.200	1.20
Lot number: LAXMO-003-1.2-RAM			

In a small conductive container was placed MoO$_3$ (250 mg) and L-ALEX (146 mg). The container was capped with a rubber stopper. The container was attached with a metallic hose clamp which was used to ground the system. The bottle was placed in the LabRAM mixer, grounded and the mixing rate was set as follows: 10% intensity for a period of 10 seconds and at 30% intensity for 30 seconds. The mixing was done in remote control. Visually, the mixture appeared homogeneous. The Al/MoO$_3$ nanothermite was placed in a conductive container and stored. Another preparation of Al/MoO$_3$ nanothermite (Lot number: **LAXMO-004-1.2-RAM**) was prepared following the same procedure but starting from 650 mg of MoO$_3$ and 378 mg of L-ALEX to yield 1.028 g of nanothermite. The time of mixing at 30% intensity was also increased to 60 seconds.

3.2.3   Al/Bi$_2$O$_3$ nanothermite

2Al + Bi$_2$O$_3$ → Al$_2$O$_3$ + 2Bi			
	FW	**Weight (mg)**	**Mmol**
Al	26.982	39.5	1.288
Actual Al		45.0	
Bi$_2$O$_3$ (200 nm)	465.959	250.0	0.537
Total mass		295.0	
Mass Ratio $_A$		0.158	
Mol Ratio $_A$			2.400
Mass Ratio $_s$		0.116	
Mol Ratio $_s$			2.000
Equivalence ratio ϕ		1.200	1.20
Lot number: LAXBI-004-1.2-RAM			

In a small conductive container was placed Bi$_2$O$_3$ (250 mg) and L-ALEX (45 mg). The container was capped with a rubber stopper. The container was attached with a metallic hose clamp which was used to ground the system. The bottle was placed in the LabRAM mixer, grounded and the mixing rate was set as follows: 10% intensity for a period of 10 seconds and at 30% intensity for 30 seconds. The mixing was done in remote control. Visually, the mixture appeared homogeneous. The Al/Bi$_2$O$_3$ nanothermite was placed in a conductive container and stored. Another preparation of Al/Bi$_2$O$_3$ nanothermite (Lot number: **LAXBI-005-1.2-RAM**) was prepared following the same procedure but starting from 850 mg of Bi$_2$O$_3$ and 153 mg of L-ALEX to yield 1.003 g of nanothermite. The time of mixing at 30% intensity was also increased to 60 seconds.

3.3   Impact, friction and electrostatic discharge sensitivity (ESD) test

The results for sensitivity to impact are the same for all three nanothermites. All three nanothermites are insensitive to impact; the value obtained is higher than 80 Joules.

The results for the sensitivity to friction are very different. For the nanothermite Al/CuO, single ignition was observed at 360 N and is therefore not very sensitive to this stimulus. One could observe on the ceramic plate and sample holder, the reddish color of metallic copper produced by the reaction (Fig.10). The nanothermite Al/MoO$_3$ can be considered as moderately sensitive since ignition reactions occur at 160 N. The nanothermite Al/Bi$_2$O$_3$ is by far the most sensitive with ignition reactions accompanied with loud noise at value below 5 N and probably close to 1 N, which makes this nanothermite very sensitive to friction.

Figure 10: Ceramic plate of the friction sensitivity test after reaction with Al/CuO nanothermite

Results for sensitivity to electrostatic discharge (ESD) were performed on open cell. For the nanothermite Al/CuO ignition occurs at energy of 0.056 J. As for the sensitivity to friction test, we can observe the reddish metallic copper formed on the sample holder and the needle during the reaction (Fig. 11).
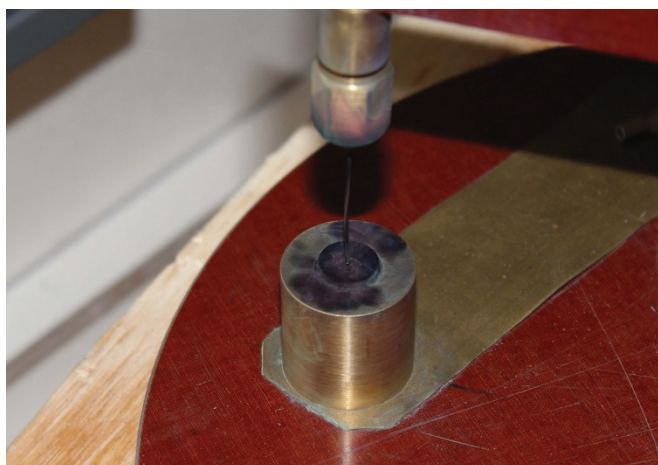
Figure 11: Setup for ESD test after ignition of Al/CuO nanothermite

The other two nanothermites, Al/MoO$_3$ and Al/Bi$_2$O$_3$ are much more sensitive to electrostatic discharge. By adjusting the voltage to the lowest value possible to observe a spark (3 kV) corresponding to energy of 1.5 mJ, there is ignition reaction for both nanothermites. In addition, as the sensitivity to friction test, the nanothermite Al/Bi$_2$O$_3$ reacts violently with powerful sound to electrostatic discharge and we found support sample broken into pieces (Fig. 12).
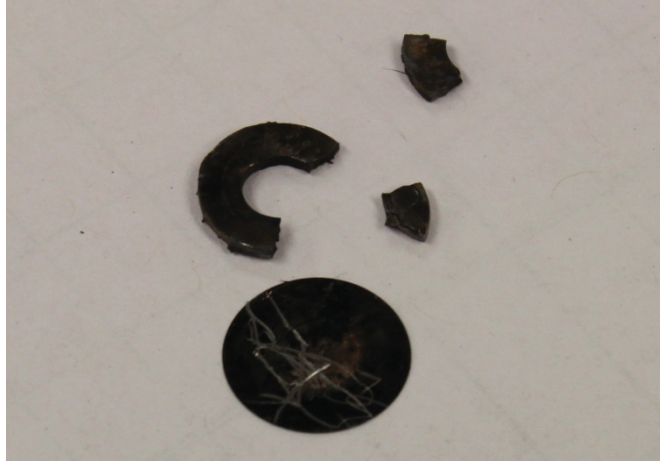
Figure 12: Sample holder after reaction to ESD for the Al/Bi$_2$O$_3$ nanothermite

3.4 Laser ignition test

One of the main objectives of this preliminary study was to test that aluminum-based nanothermites could be ignited by irradiation with low power laser. The three nanothermites Al/CuO, Al/MoO$_3$ and Al/Bi$_2$O$_3$ were submitted laser ignition tests. In Fig. 13 is shown an example of the laser ignition of Al/MoO$_3$ nanothermite with a blue laser at an output of 150 mW. We observe in this case, an ignition delay of 36 msec. All detailed results of these tests and the experimental procedure can be found in the technical report written by Tommy Ringuette. The results of these initial tests are very interesting and show the enormous potential of aluminum-based nanothermites for use as ammunition primers.
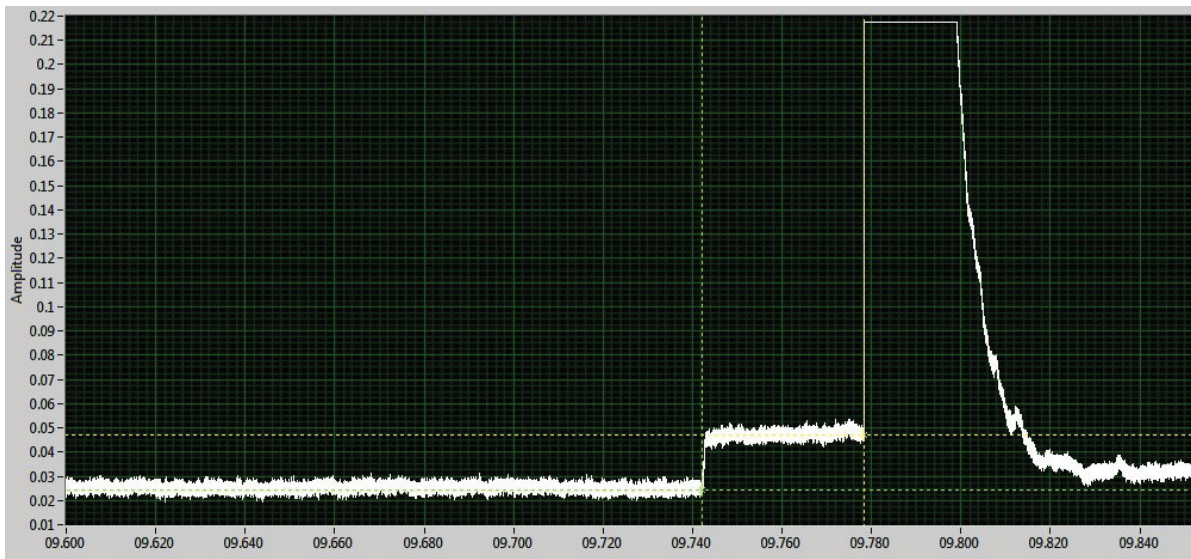

Figure 13: Example of laser ignition of Al/MoO$_3$ nanothermite with ignition delay of 36 msec

DRDC-RDDC-2014-C39

4. *Future projects and conclusion*

4.1 Thermal characterization of nanothermites

The first characteristics of an energetic material that must be performed are related to safety aspects. This is what has been done with nanothermites by obtaining their level of sensitivity to friction, impact and electrostatic discharge. What has not been done in this project is the thermal characterization of nanothermites.

The use of differential scanning calorimetry would provide ignition temperatures and the activation energies of nanothermites [9]. Thermogravimetric analysis would also be useful to evaluate the thermal stability of nanothermites [12-14].

4.2 Variation in composition of nanothermites

The objective of the first phase of this project was to get a quick overview of possibilities offered by nanothermites as primers and assess their ignition with a low energy laser. The possibilities are countless for the types of nanothermite mixtures. It is known that the particle size of aluminum has a huge importance in the final characteristics of a nanothermite. For the purposes of this project and the time available, we limited ourselves to the use of only one type of aluminum nanopowder, L-ALEX with a size of 90-110 nm. As we have seen in its description this aluminum is coated with palmitic acid. It would be interesting to evaluate other nanothermites mixtures obtained from aluminum with different coatings such as Viton, nitrocellulose or even without coating. The type of coating may have a significant impact on the characteristics of the final product [14-16]. We can also consider using two different aluminum powders with different size and/or coating in a nanothermite to modulate the characteristics that are desired [17].

There are very few examples in the literature where are varied the size of the metal oxide powders to modulate the characteristics of nanothermite. However, it is possible to use mixtures of different metal oxides with a powder of aluminum and thereby obtain nanothermites with various properties. As an example, we know that nanothermite consisting of iron oxide (Fe_2O_3) is less sensitive to ignition than a bismuth oxide (Bi_2O_3) nanothermite. The incorporation of Fe_2O_3 in a thermite made of Bi_2O_3 will slow down the reaction and will prolonged interaction with the propellant for specific applications [16].

As we can see, there are several settings that can be modified that would allow adjusting the physical characteristics of nanothermites for specific applications. Among the main factors are: the size of aluminum particles, the type of coating, the combination of different particle size, the type and size of the metal oxide particles, the use of different metal oxides, the equivalence factor φ, the mixing technique use to prepare nanothermites and of course a combination of several of these factors. Further studies on different formulations of nanothermites are required to meet specific applications that we want to implement.

References

[1] Ajayan, P. M., Terrones, M., de la Guardia, A., Huc, H., Grobert, N., Wei, B. Q., Lezec, H., Ramanath, G., and Ebbesen, T. W., "Nanotubes in a Flash—Ignition and Reconstruction", *Science* 296: 705 (2002).

[2] Krishna, V., Stevens, N., Koopman, B., and Moudgil, B., "Optical heating and rapid transformation of functionalized fullerenes", *Nature Nanotechnology* 5: 330-334 (2010).

[3] Semenov, K. N., Charykov, N. A., Keskinov, V. N., "Fullerenol Synthesis and Identification. Properties of the Fullerenol Water Solutions", *J. Chem. Eng. Data* 56: 230–239 (2011).

[4] Kokubo, K., Shirakawa, S., Kobayashi, N., Aoshima, H., and Oshima. T., "Facile and Scalable Synthesis of a Highly Hydroxylated Water-Soluble Fullerenol as a Single Nanoparticle", *Nano Res*. 4(2): 204-215 (2011).

[5] Mirkov, S. N., Djordjevic, A. N., Andric, N. L., Andric, S. A., Kostic, T. S., Bogdanovic, G. N., Vojinovic-Miloradov, M. B., and Kovacevic, R. Z., "Nitric oxide-scavenging activity of polyhydroxylated fullerenol, $C_{60}(OH)_{24}$", *Nitric Oxide* 11: 201–207 (2004).

[6] http://science.widener.edu/~schultz/c60br24.html

[7] Grebowski, J., Krokosz, A., and Puchala, M., "Membrane fluidity and activity of membrane ATPases in human erythrocytes under the influence of polyhydroxlated fullerenes", *Biochimica and Biophysica Acta (BBA)-Biomembranes* 1828(2): 241-248 (2013).

[8] Adams, C., "Explosive/energetic fullerenes" U.S. Patent 7 025 840, 11 April 2006.

[9] Puszynski, J. A., Bullian, C. J., and Swiatkiewicz, J. J., "Processing and Ignition Characteristics Of Aluminum-Bismuth Trioxide Nanothermite System", *Journal of Propulsion and Power*, 23(4): 698-706 (2007).

[10] Pantoya, M., and Granier, J. J., "Combustion Behavior of Highly Energetic Thermites: Nano versus Micron Composites", *Propellants, Explosives and Pyrotechnics*, 30(1): 53-62 (2005).

[11] Fischer, S.H., Grubelich, M.C., "A survey of combustible metals, thermites, and intermetallics for pyrotechnic applications", *Report# SAND--95-2448C; CONF-960717—4*, AIAA/ASME/SAE/ASEE joint propulsion conference and exhibit, Orlando, FL (United States), 1-3 Jul 1996.

[12] Wang, J., Hua, A., Persic, J., Wen, J. Z., and Zhou, Y. N., "Thermal stability and reaction properties of passivated Al/CuO nano-thermite", *Journal of Physics and Chemistry of Solids*, 72: 620–625 (2011).

[13] Stamatis, D., and Dreizin, E. L., "Thermal Initiation of Al-MoO3 Nanocomposite Materials Prepared by Different Methods", *Journal of Propulsion and Power*, 27(5): 1079-1087 (2011).

[14]   Kappagantula, K. S., Farley, C., Pantoya, M. L., and Horn, J., "Tuning Energetic Material Reactivity Using Surface Functionalization of Aluminum Fuels", *The Journal of Physical Chemistry C*, 116: 24469–24475 (2012).

[15]   Foley, T., Pachero, A., Malchi, J., Yetter, R., and Higa, K., "Development of Nanothermite Composites with Variable Electrostatic Discharge Ignition Tresholds", *Propellants, Explosives and Pyrotechnics*, 32(6): 431-434 (2007).

[16]   Bulian, C. J., Puszynski, J. A., and Swiatkiewicz, J. J., "Tunability of Nanoenergetic Materials" Retrieved March 27, 2013, from: http://www.nt.ntnu.no/users/skoge/prost/proceedings/aiche-2008/data/papers/P128319.pdf

[17]   Moore, K., Pantoya, M. L., and Son, S. F., "Combustion Behaviors Resulting from Bimodal Aluminum Size Distribution in Thermites", *Journal of Propulsion and Power*, 23(1): 181-185 (2007).